

FIRST ANALYSIS OF THE SPACE CHARGE EFFECTS ON A THIRD ORDER COUPLED RESONANCE

G. Franchetti, GSI, Darmstadt, Germany

S. Gilardoni, A. Huschauer, F. Schmidt, R. Wasef, CERN, Geneva, Switzerland

Abstract

The effect of space charge on bunches stored for long term in a nonlinear lattice can be severe for beam survival. This may be the case in projects as SIS100 at GSI or LIU at CERN. In 2012, for the first time, the effect of space charge on a normal third order coupled resonance was investigated at the CERN-PS. The experimental results have highlighted an unprecedented asymmetric beam response: in the vertical plane the beam exhibits a thick halo, while the horizontal profile has only core growth. The quest for explaining these results requires a journey through the 4 dimensional dynamics of the coupled resonance investigating the fixed-lines, and requires a detailed code-experiment benchmarking also including beam profile benchmarking. This proceeding gives a short summary of the experimental results of the 2012 PS measurements, and address an interpretation based on the dynamics the fixed-lines.

INTRODUCTION

Space charge induced emittance growth and beam loss can be divided into two big classes. The beam loss deriving from the incoherent effects of space charge on lattice nonlinearities (this proceeding), and the beam loss that may arise from the growth of the coherent modes self-consistently excited by the space charge [1].

The incoherent effects of space charge in coasting beams create an emittance growth when the space charge detuning overlaps a machine resonance. However, the incoherent space charge tune-shift also stabilizes the emittance growth by bringing particles out of the resonance as they grow in transverse amplitude. The space charge induced beam loss in a nonlinear machine becomes dramatic for bunched beams when the synchrotron motion and space charge induce a periodic crossing of a machine resonance. A single resonance crossing in a conventional RF bucket with synchrotron tune of $Q_s \sim 10^{-2}$ produces a small emittance growth because of the relatively fast resonance crossing, but the cumulative effect arising from repeated resonance crossing, more than 300-400 crossing, makes large impact creating a beam diffusion to large transverse amplitudes, hence may lead to a steady beam loss over all the storage time.

For one dimensional resonances the mechanism leading to emittance growth and beam loss is explained in terms of instantaneous stable islands in the two-dimensional phase space and their crossing the particle orbits because of the combined effect of space charge and synchrotron motion Ref. [2]. This mechanism requires a long term storage, which typically corresponds to a number of turns equivalent to 100 or more synchrotron oscillations. Experimental and

numerical studies on beam survival and emittance growth in this regime have investigated the one dimensional resonance $4Q_x = 25$ in Ref. [3], and $3Q_x = 13$ in Ref. [4]. The relevance of these studies is significant for SIS100 [5], and for LIU [6] at CERN, as well as for all accelerators operating with high intensity beams in regimes of long term storage.

RESULTS AND DISCUSSION

Coupled nonlinear resonances, of which the simpler class is the $Q_x + 2Q_y = N$, leads to significant difficulties in presence of space charge, and experimental studies are mandatory to unravel the complex dynamics. The effect of space charge on these type of resonances was studied in the CERN-PS in 2012 for the resonance $Q_x + 2Q_y = 19$. In this proceeding we present a short summary of the full experiment analysis. A more comprehensive presentation of the experimental results and discussion is part of a future publication.

In the experiment, in a resonance-free region of the tune diagram the third order resonance $Q_x + 2Q_y = 19$ was excited with sextupoles with strength of $K_3 \approx 0.015 \text{ m}^{-2}$. The experimental campaign used a beam with 55×10^{10} proton per bunch, which produced an incoherent space charge tune-shift of $\Delta Q_x \approx -0.05$, $\Delta Q_y \approx -0.07$. The beam was stored for $\sim 0.5 \times 10^6$ turns, i.e. 1.1 seconds at an energy of 2 GeV, and beam profile measurements were taken at the beginning and at the end of the storage time. For several machine tunes, initial and final beam profiles were compared with the finding of an unexpected beam response to the distance from the resonance. When the space charge tune-spread overlaps the third order resonance and the machine tune is close to the resonance without beam loss, the beam profiles evolve differently in the transverse planes: in horizontal plane the beam exhibits core growth, whereas in the other plane a large halo is formed. This is shown in Fig. 1a,b for the tunes $Q_{x0} = 6.104$, $Q_{y0} = 6.476$. The asymmetry of the beam profile is quite evident and shows that a new and more complex dynamics is driving the beam halo formation. In the picture are also shown the profiles from computer simulation as obtained from MADX, and MICROMAP (see Ref. [7] for a general code benchmarking discussion). Figure 1c shows the overall beam response in the experiment. The profiles in Fig. 1a,b correspond to the largest emittance growth.

The explanation of the halo-core finding can be approached starting with a detuning analysis. The theory of the resonances (see Ref. [8,9]) shows that the more convenient quantity to measure the distance from the third order resonance is

$$\Delta_{r0} = Q_{x0} + 2Q_{y0} - 19.$$

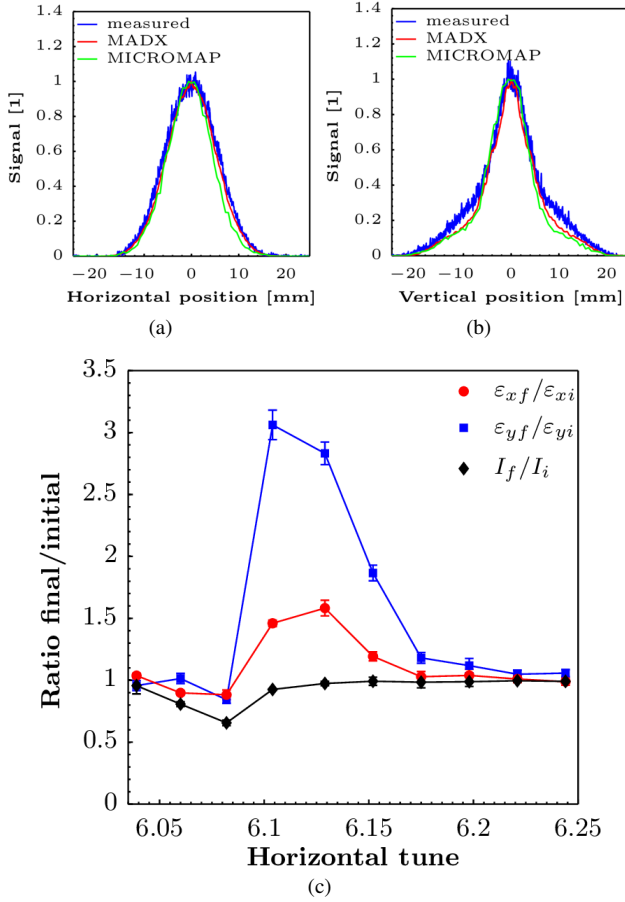


Figure 1: Part a, and b: horizontal and vertical beam profiles after 1.1 second storage of the beam in the CERN-PS. The asymmetry of the beam response is evident. In part c is shown the full beam response to all working points investigated.

When $\Delta_{r0} = 0$ the machine tunes sit on the resonance. This definition valid for the machine tunes can be extended to any arbitrary particle, hence it becomes $\Delta_r = Q_x + 2Q_y - 19$, where now the tunes Q_x, Q_y are the effective tunes experienced by a test particle, which is affected by space charge, chromaticity, and any other effects. If we call $\Delta Q_{sc,x}(X, Y), \Delta Q_{sc,y}(X, Y)$ the amplitude dependent detuning created by space charge for a particle with amplitudes X, Y , the distance from the resonance reads

$$\Delta_r = \Delta_{r0} + \Delta Q_{sc,x}(X, Y) + 2\Delta Q_{sc,y}(X, Y). \quad (1)$$

Therefore one can use this relation for a first order search of the amplitudes of the resonant particles.

Given the machine tunes Q_{x0}, Q_{y0} we find Δ_{r0} , and the resonant transverse amplitudes are found as the X, Y which satisfy the equation $\Delta_r = 0$.

The quantity Δ_r becomes therefore dependent from X, Y and can be regarded as a resonance detuning that incorporates the coupled character of the resonance $Q_x + 2Q_y = 19$. In Fig. 2 the two curves show the dependence of Δ_r for two

types of particle amplitudes. The red curve is obtained for amplitudes type $(X, 0)$, while the black curve is obtained for amplitudes $(0, Y)$. The horizontal line of height $\Delta_r = 0$ intercepts the two curves at the resonant amplitudes, which in our case are $X \sim 5\sigma_x$, and $Y \sim 4\sigma_y$.

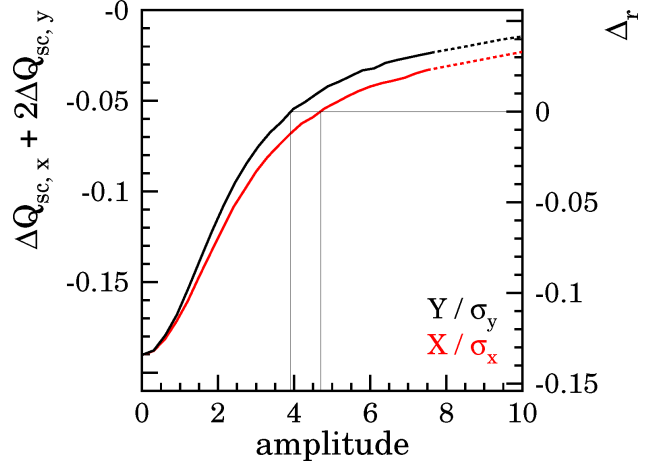


Figure 2: Resonance detuning Δ_r as function of the particle amplitude.

From the phenomena of periodic resonance crossing we expect that particle diffusion is not exceeding the outer position of the “resonant particles”, which is $X \sim 5\sigma_x$, and $Y \sim 4\sigma_y$. However, a comparison with a multi-particle simulation in absence of chromaticity, shows that no halo with amplitude $X \sim 5\sigma_x$ is found.

By adding the chromaticity to Eq. (1) we can investigate the role of the chromaticity on the resonant amplitudes, for example for particles with maximum $\delta p/p$, and construct an equivalent graphic of Fig. 2. Adopting the same procedure as previously described, we can search for the resonant particles at largest amplitudes (condition $\Delta_r = 0$). We find that the halo predicted by this analysis is $X > 9\sigma_x$, and $Y \sim 9\sigma_y$. Once more, this result contradicts the experimental findings, in which the halo is found at $Y \approx 5.5\sigma_y$.

INTERPRETATION WITH THE FIXED LINES

The explanation of the beam profile observed and retrieved from simulations in Fig. 1 goes beyond the detuning analysis, and have to be searched into the effects created by the 4D coupled dynamics. The analogous of the fixed-points is now the fix-lines [9–11]. The analytic form of these lines (or resonant tori) is parameterized as

$$x = \sqrt{\beta_x a_x} \cos(-2t - \alpha + \pi M), y = \sqrt{\beta_y a_y} \cos(t). \quad (2)$$

The coordinates x', y' are readily derived from Eq. (2). The fixed-line emittances a_x, a_y are determined by the distance to the resonance Δ_{r0} . The variable t parameterizes the fixed-line. In absence of space charge and of nonlinear detuning, the fixed-line has the largest extension in the y direction, and in particular the ratio of the fixed-line invariants takes the

value of $a_y/a_x = 8$ when a_y is maximum (see Ref. [10]). The coefficient M is 0, or 1 according to the condition of existence of the fixed line. In Fig. 3 we shows an example of

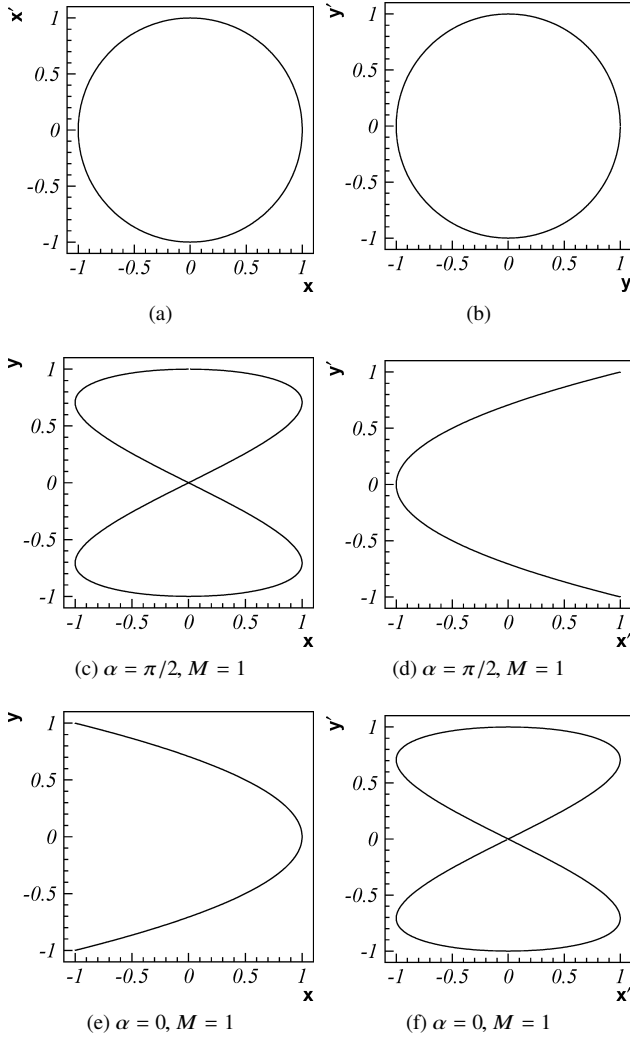


Figure 3: Fixed-line projections in normalized coordinates. The parameters in Eq. (2) are indicated in each picture. Note that the topology of the $x - y$ projection of a fixed-line depends substantially on the angle α .

the shape of these lines plotted in normalized coordinates. It is visible that the $x - y$ projection of the resonant particle on the fixed-line have a special form which can be easily identified. The dependence of α makes the shape “C” and the shape “8” exchangeable. Practically the parameter α is the phase of the driving term of the third order resonance, and in our case it depends on the location of the sextupoles used to excite the resonance with respect to the observation point along the machine (the flying wire position). Also on the interplay of space charge with the resonant dynamics is relevant, but the theory of fixed-lines with space charge is not available, hence only a numerical investigation can be presented.

The investigation of the role of the fixed-lines in the bunched beam is first carried out by freezing artificially

the longitudinal motion in the simulation modeling the experimental beam profiles of Fig. 1, and by constructing a tune footprint of a set of test particles. The resonant particles are easily identified as the FFT method used to retrieve the single particle nonlinear tunes Q_x, Q_y , locks the single particle tunes of resonant particles to the line $Q_x + 2Q_y - 19 = 0$. We then plot the $x - y$ projection of the resonant orbits and compare it with the $x - y$ projections in Fig. 3 searching for indications of a fixed-lines dynamics. In part a of Fig. 4 we

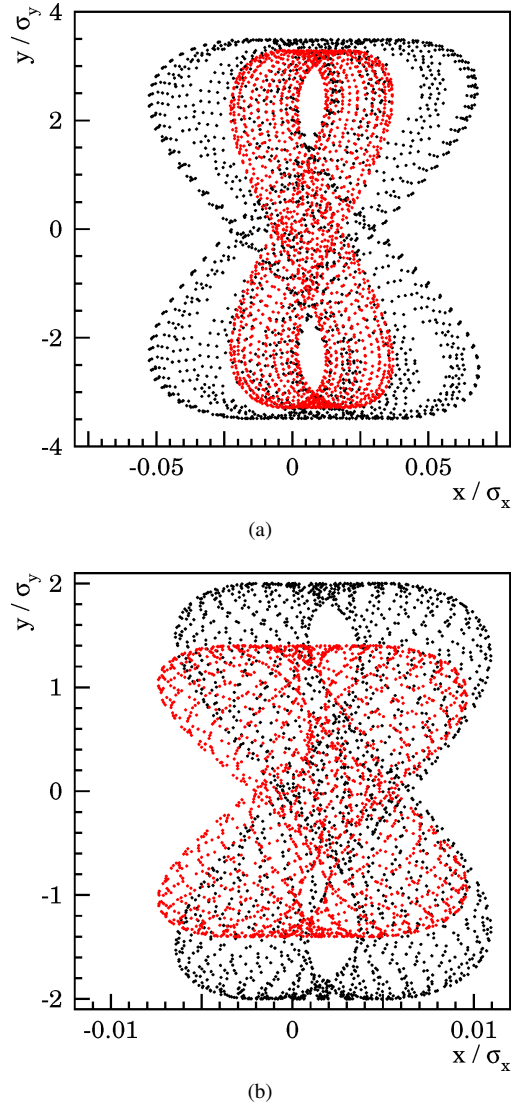


Figure 4: Part a). $x - y$ projection of the two largest resonant orbits at $z = 0\sigma_z$; Part b). The two largest resonant orbits now at $z = 1.5\sigma_z$.

show two resonant orbits for test particles located at $z = 0\sigma_z$. The topology of the orbit projection leaves no doubt that we see two particles locked to two distinct fixed lines having the “8” shape in $x - y$ projection. The asymmetric form of the orbits is remarkable although the resonant particle is not sitting exactly on the fixed-line. This result simply shows that the presence of the beam space charge detuning does not destroy the dynamics that creates the fixed-lines.

By repeating the analysis for particles at $z = 1.5\sigma_z$ we can visualize the resonant orbits at a location of the bunch with smaller transverse space charge. These resonant orbits are shown in part b of Fig. 4. Even in this case we clearly distinguish in the resonant orbits the pattern of the fixed-lines. The aspect ratio is now different, and the extension of the orbits is smaller.

This pattern of the extension of the fixed-lines along the bunch is consistent with the studies on one dimensional resonances. In Ref. [2] it is shown that the frozen transverse islands have the maximum size and their fixed-points have maximum amplitudes at longitudinal positions $z = 0$. For other longitudinal position within the bunch the fixed-points are found at smaller amplitudes. Eventually at locations enough far away from the bunch center, the fixed-points merge to the transverse origin and disappear. This pattern is at the base of the periodic resonance crossing mechanism. Figure 4a,b convey the same information as they show that instantaneous fixed-lines have amplitude function of the longitudinal particle coordinate z in the bunch reference frame. This pattern which exhibits the largest fixed-lines at $z = 0\sigma_z$, with amplitude decreasing for increasing the longitudinal amplitude, will create phenomena of periodic crossing of the fixed-lines. This can be seen in Fig. 5 where the evolution of the single particle emittance is shown during one synchrotron oscillation. The scattering of the invariant is clearly visible with 4 kicks per synchrotron oscillation.

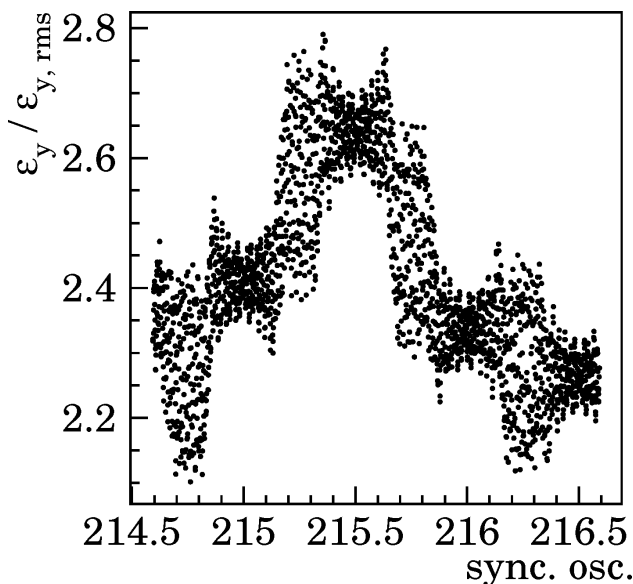


Figure 5: Emittance of one test particle during storage. The picture reveals the 4 kicks exerted by the fixed-lines during one synchrotron oscillation.

CONCLUSION AND OUTLOOK

In this proceeding we shortly summarize the main findings of the PS experiment performed in 2012. We find a simulation evidence that the dynamics creating the halo is determined by the fixed-lines. We find that the fixed-lines

change amplitude according to the strength of the instantaneous space charge tune-spread, which depends on the particle longitudinal position within the bunch. This induces a phenomena of periodic crossing of the fixed-lines with the particle orbit. Scattering phenomena are found in the simulation as a clear trace of this fundamental mechanism. The asymmetry of the measured beam response is a result of the asymmetric shape of the instantaneous fixed-lines.

It remains open and is not discussed in this proceeding the influence of the many fixed-lines on the particle motion, and the explanation of why the halo in the experiment extends only up to $5.5\sigma_y$, although simulations clearly show the existence of many fixed-lines which extends on a larger surface, reaching up to $9\sigma_y$ when the effect of the chromaticity is included. If it is possible to identify which is the fixed-line of relevance for the scattering mechanism, it will be possible to predict the extension of the halo without actually running the very demanding multi-particle simulations. The understanding of this mechanism is also of relevance on the issue of the resonance compensation, which attempt was already presented in HB2014 in Ref. [12].

The discussion of all these aspects as well as of the open question here presented is left to a future publication.

ACKNOWLEDGMENT

"The research leading to these results has received funding from the European Commission under the FP7 Research Infrastructures project EuCARD-2, grant agreement no.312453".

REFERENCES

- [1] I. Hofmann, in *Proc. HB'16*, Malmö, Sweden, July 2016, paper THPM1X01, this conference. .
- [2] G. Franchetti and I. Hofmann, *Nucl. Instr. and Meth. A* **561**, (2006), pp.195-202.
- [3] G. Franchetti, I. Hofmann, M. Giovannozzi, M. Martini, E. Métral, *Phys. Rev. ST Accel. Beams* **6**, 124201 (2003); E. Métral, G. Franchetti, M. Giovannozzi, I. Hofmann, M. Martini, and R. Steerenberg, *Nucl. Instr. and Meth. A* **561**, (2006), 257-265.
- [4] G. Franchetti, O. Chorniy, I. Hofmann, W. Bayer, F. Becker, P. Forck, T. Giacomini, M. Kirk, T. Mohite, C. Omet, A. Parfenova, and P. Schuett, *Phys. Rev. ST Accel. Beams* **13**, 114203 (2010).
- [5] P. Spiller and G. Franchetti, *Nucl. Instrum. Methods Phys. Res., Sect. A* **561**, 305 (2006).
- [6] J. Coupard *et al.*, "LHC Injectors Upgrade, Technical Design Report, Vol. I: Protons", LIU Technical Design Report (TDR), CERN-ACC-2014-0337.
- [7] F. Schmidt *et al.*, "Code Bench-Marking for Long-Term Tracking and Adaptive Algorithms", in *Proc. HB'16*, Malmö, Sweden, July 2016, paper WEAM1X01, this conference.
- [8] A. Schoch, "Theory of Linear and Non-Linear Perturbations of Betatron Oscillations in Alternating Gradient Synchrotrons", CERN 57-21 (Proton Synchrotron Division), Section 14 (1958).

- [9] G. Franchetti and F. Schmidt, “Extending the Nonlinear-Beam-Dynamics Concept of 1D Fixed Points to 2D Fixed Lines”, *Phys. Rev. Lett.* **114**, 234801 (2015).
- [10] G. Franchetti and F. Schmidt, “Fix-lines and stability domain in the vicinity of the coupled third order resonance”, <http://arxiv.org/abs/1504.04389>
- [11] F. Schmidt, “Untersuchungen zur dynamischen Akzeptanz von Protonenbeschleunigern und ihre Begrenzung durch chaotische Bewegung”, PhD thesis, DESY HERA 88-02 (1988).
- [12] G. Franchetti, S. Aumon, F. Kesting, H. Liebermann, C. Omet, D. Ondreka, and R. Singh, GSI, S. Gilardoni, A. Huschauer, F. Schmidt, and R. Wasef, CERN in *Proc. of HB’14*, East Lansing, USA. paper THO1LR03. p. 330.